

Vibrational thermodynamics: coupling of chemical order and size effects

Dane Morgan[†], Axel van de Walle[†], Gerbrand Ceder[†], Jeffrey D Althoff[‡] and Didier de Fontaine[‡]

[†] Department of Materials Science and Engineering, Massachusetts Institute of Technology, Cambridge, MA 02139, USA

[‡] Department of Materials Science and Mineral Engineering, University of California, Berkeley, CA 94720, USA

Received 16 September 1999, accepted for publication 1 March 2000

Abstract. The effects of chemical order on the vibrational entropy have been studied using first-principles and semi-empirical potential methods. Pseudopotential calculations on the Pd₃V system show that the vibrational entropy decreases by $0.07k_B$ upon disordering in the high-temperature limit. The decrease in entropy contradicts what would be expected from simple bonding arguments, but can be explained by the influence of size effects on the vibrations. In addition, the embedded-atom method is used to study the effects of local environments on the entropic contributions of individual Ni and Al atoms in Ni₃Al. It is found that increasing numbers of Al nearest neighbours decreases the vibrational entropy of an atom when relaxations are not included. When the system is relaxed, this effect disappears, and the local entropy is approximately uniform with increasing number of Al neighbours. These results are explained in terms of the large size mismatch between Ni and Al. In addition, a local cluster expansion is used to show how the relaxations increase the importance of long-range and multisite interactions.

1. Introduction

The role of vibrational thermodynamics in phase stability is still poorly understood. Traditionally, the effects of vibrations have not even been considered in theoretical phase stability studies, which focused primarily on substitutional influences [1–4]. There is growing evidence, both experimental [5–12] and theoretical [13–24] that vibrational thermodynamics can have a significant influence on phase diagrams.

Unfortunately, at present there are only the beginnings of a qualitative understanding of how differences in vibrational thermodynamics arise. In real systems, various mechanisms such as volume differences, bond type differences, internal strain effects, and defect structures (impurities, grain boundaries, etc) can all contribute to the vibrational thermodynamics, making it difficult to separate out the contributions of each. An advantage of computational approaches is that it is possible to manipulate the system being studied so as to isolate different mechanisms, for example, by removing thermal expansion or restricting internal relaxations. In this paper we will use computational approaches to study how relaxations and bonding changes between different chemical orderings influence vibrational entropies.

The key results can be summarized as follows. First-principles pseudopotential calculations for the vibrational entropy of Pd₃V indicate that upon disordering the *DO*₂₂ phase the vibrational entropy *decreases* by $0.07k_B$ [25]. This is somewhat surprising since the *DO*₂₂ phase is expected to have stiffer bonds, and therefore a lower vibrational entropy,

than the disordered phase. More detailed analysis shows that despite the small size mismatch between Pd and V there is significant relaxation allowed in the disordered phase that is not possible in the DO_{22} structure. The different relaxations occur because any given disordered configuration has much lower symmetry than the DO_{22} phase (although, when the occupations are thermodynamically averaged, the averaged disordered phase has higher symmetry than DO_{22}). It is shown that the greater relaxation allows a stiffening of the Pd–V bonds, which leads to the lowering of the entropy with disordering.

When the embedded-atom method is used to calculate a local vibrational entropy for each atom in Ni_3Al , it is found that for an unrelaxed crystal the local entropy increases with increasing numbers of Al nearest neighbours, but that this trend disappears when the proper relaxations are included [26]. The effects of the relaxations are understood in terms of the large size mismatch between the Ni and Al atoms. When no relaxations are allowed, the large Al crowd the atoms they surround, reducing the vibrational entropy. When relaxations are allowed, the large Al push each other away, which reduces crowding and does not change the vibrational properties of a surrounded atom very strongly. A local cluster expansion is used to analyse the relaxation effects in more detail, and the results show that the relaxations increase the importance of long-range and multisite interactions.

This paper is arranged as follows. Section 1 contains the introduction. Section 2 contains the qualitative framework in which we will analyse the calculations. A Lennard-Jones potential is used to demonstrate how the qualitative picture is realized in a simple system. Section 3 discusses first-principles calculations of the vibrational entropy difference between DO_{22} and disordered Pd_3V . Section 4 discusses embedded-atom method calculations of the influence of local environments on the local vibrational entropy in Ni_3Al . Finally, section 5 gives a summary and conclusions.

2. Qualitative framework

First we will discuss a simple qualitative picture of the effects of changing chemical order on the vibrational thermodynamics. We will restrict the discussion to various lattice decorations of a fixed parent lattice at a fixed composition. In the harmonic approximation [27], the vibrational thermodynamics of a given structure are determined by its dynamical matrix, which in turn is given by the force constant matrix and the masses. At a fixed composition and high temperatures the masses contribute a constant term to the vibrational thermodynamics and can therefore be ignored when considering differences [2]. Changes in the vibrational thermodynamics between different lattice decorations must therefore come from changes in the proportions of different force constants, or changes in their actual values.

A sensible starting model for how the force constants are affected by chemical order is what we will call the ‘bond-proportion model’. This model assumes that each type of bond carries with it an approximately fixed force constant, and that changes in the force constants with chemical order are due primarily to changes in the proportions of different types of bonds. This sort of model is often used to give a simple starting Hamiltonian from which more elaborate theoretical calculations are tractable [14, 28].

If this bond-proportion model is accurate, even qualitatively, there are certain implications for the behaviour of vibrational entropies. For example, consider an ordered compound, and compare it to the pure elements from which it is made. As a first approximation the force constants between unlike species are given by the harmonic mean of the force constants between like species. For bonding of this type the bond-proportion model predicts very little change in the vibrational thermodynamics upon disordering [14]. For a strongly ordering material it is to be expected that bonds between unlike species are more stable, and therefore have somewhat

stiffer force constants than the harmonic mean of the bonds between like species. The stiffer average force constants would generally cause the ordered phase to have a lower vibrational entropy than the average of the pure elements (which have only like neighbour bonds). Define the vibrational formation entropy of a binary compound $A_{1-c}B_c$ by

$$\Delta S_{\text{form}} = S_{\text{ord}} - (1 - c)S_A - cS_B \quad (1)$$

where S_{ord} , S_A , and S_B are the vibrational entropies of the ordered, pure A, and pure B materials, respectively. The above arguments show that the bond-proportion model predicts that for an ordering alloy the vibrational formation entropy would be negative. Another implication of the bond-proportion model is that for an ordering alloy, the disordered phase will have a larger vibrational entropy than an ordered phase of the same composition. This follows from the fact that the disordered phase has fewer unlike neighbour bonds associated with stiff force constants than the ordered phase.

Unfortunately, neither experiments nor direct first-principles calculations support the predictions of the bond-proportion model in general. Calculations of the high-temperature limit of ΔS_{form} based on experimentally measured force constants and densities of states show that many ordered compounds have positive values of ΔS_{form} [12]. Furthermore, first-principles calculations on the Cu–Au system found positive values of ΔS_{form} for all the ordered structures studied [23]. These results are not consistent with the bond-proportion model.

Experimental measurements for a number of systems [6–9, 11] have consistently found that the vibrational entropy increases with disordering, which matches the predictions of the bond-proportion model. On the other hand, first-principles results for Ni_3Al , which is a very strongly ordered compound, essentially show no change in entropy between the ordered and disordered phases [22].

We propose that to explain, even qualitatively, the changes in vibrational entropy, one must go beyond a simple bond-proportion model and incorporate size effects. By size effects we mean the effects on the force constants that are associated with compression and stretching of the bonds. Size effects are not included in the simple bond-proportion model, where all bonds are considered fixed in their strength. For example, if elements A and B have very different sizes, there is no reason to expect A–A bonds to have similar force constants in A and B rich environments, since the A–A bonds will be of very different lengths in the two cases.

An intuitive understanding of the interplay between size and bond-type effects can be obtained by considering a simple nearest-neighbour Lennard-Jones potential. This potential has been used to calculate the change in the value of the vibrational thermodynamics between ordered $L1_0$ and a fcc disordered phase in the harmonic approximation. In the high-temperature limit the relevant thermodynamics can be calculated from the logarithmic average of the density of states ($\langle \ln \omega \rangle$), which is defined by

$$\langle \ln \omega \rangle = \int_0^\infty \ln(\omega) g(\omega) d\omega \quad (2)$$

where $g(\omega)$ is the vibrational density of states and ω is the frequency. Define the change in $\langle \ln \omega \rangle$ by $\Delta \langle \ln \omega \rangle = \langle \ln \omega \rangle_{\text{disordered}} - \langle \ln \omega \rangle_{\text{ordered}}$. The change in vibrational free energy (ΔF) and entropy (ΔS) with disordering can then be written simply as

$$\Delta F = k_B T \Delta \langle \ln \omega \rangle \quad (3)$$

$$\Delta S = -k_B \Delta \langle \ln \omega \rangle. \quad (4)$$

The disordered phase was modelled by randomly distributing A and B type atoms on a cube-shaped 256-atom supercell of fcc, where the concentration was constrained to remain at A–50 at% B. Calculations were converged to within ± 0.01 in $\langle \ln \omega \rangle$ with respect to k -points. The $L1_0$ structure was completely relaxed whereas the corresponding disordered phase was

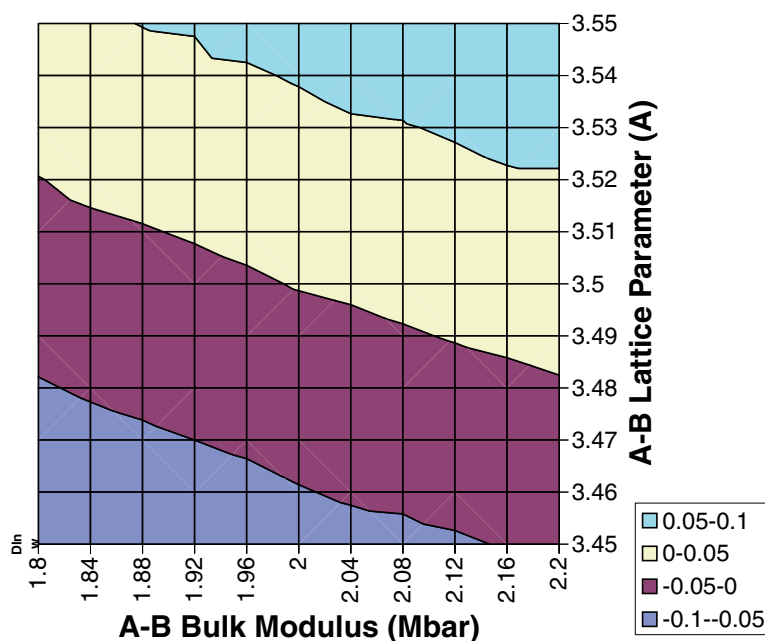


Figure 1. $\Delta\langle\ln\omega\rangle$ as a function of the effective bulk modulus and lattice parameter of the A–B bonds. A–A and B–B bonds are fixed to an effective bulk modulus of 2 Mb and lattice parameter of 3.5 Å. The calculations are all performed with a nearest-neighbour Lennard-Jones potential.

only relaxed internally, keeping the overall volume per atom fixed Ll_0 and the three supercell lattice parameters equal to each other. This removed any complications that might occur due to volume changes between the two phases. No thermal expansion effects were included. All calculations were performed using the GULP program [29].

In figure 1 the values of $\Delta\langle\ln\omega\rangle$ are plotted as a function of the bulk modulus and lattice parameter that would be obtained for an fcc structure made of A–B bonds only (this is not physically realizable but characterizes the A–B bond properties in a transparent manner). The A–A and B–B bonds are all fixed to give a bulk modulus of 2 Mb and a lattice parameter of 3.5 Å for pure A and B lattices.

Consider first the values along the horizontal line for which the A–B lattice parameter is equal to 3.5. Here all the bonds are the same length and there are no size effects, so it is expected that the bond-proportion arguments should be valid. This is seen to be the case by the fact that for softer A–B bonds one obtains $\Delta\langle\ln\omega\rangle < 0$, but for stiffer A–B bonds one obtains $\Delta\langle\ln\omega\rangle > 0$. Now consider the values along the vertical line for which the A–B bulk modulus is equal to two. Here all the bonds have the same strength, so any changes in the thermodynamics between ordered and disordered phases are due to size effects. For smaller A–B bonds the unlike bonds are stretched by the larger A–A and B–B bonds and therefore the A–B bonds are actually weaker than they would be at their equilibrium length. This causes an effect similar to what is seen for the weak A–B bonds with no size effects, and one obtains $\Delta\langle\ln\omega\rangle < 0$. Similar arguments show why larger A–B bonds yield $\Delta\langle\ln\omega\rangle > 0$. For the intermediate cases the bond-proportion and size effects both contribute. Although the nearest-neighbour Lennard-Jones potential demonstrates how vibrational thermodynamics are influenced by both size and bond effects, their complex interplay cannot be reliably investigated with such a simple model. Therefore, we now turn to more accurate potential and first-principles models.

3. First-principles study of Pd₃V

Pd₃V is a system for which one might expect the bond-proportion model to be accurate. Pd and V have a very small size mismatch [30]

$$\frac{(V_{\text{Pd}} - V_{\text{V}})}{(V_{\text{Pd}} + V_{\text{V}})/2} = 0.06$$

so size effects should not be too large. Pd₃V forms in an ordered DO_{22} structure for temperatures below 1090 K [31], so it is to be expected that Pd–V bonds will be stronger than the harmonic mean of Pd–Pd and V–V bonds. In addition, Pd and V are on either side of the transition metals in the periodic table. In general, bulk moduli tend to reach a maximum near the middle of the transition metals series. To the extent that a Pd–V bond resembles one between two elements of the middle of the transition metals series, it is to be expected that the Pd–V bonds will be stiffer than Pd–Pd or V–V bonds. Given these arguments, the bond-proportion model predicts that the vibrational entropy should increase upon disordering Pd–V, since fewer Pd–V bonds are present in the disordered phase.

First-principles methods have been used to calculate the vibrational thermodynamics of a few different structures of the Pd₃V system. Calculations have been performed with the quasiharmonic method [27], which extends the harmonic method to approximately include anharmonic terms by allowing volume dependent frequencies. All the entropy values quoted for Pd₃V were calculated in the high-temperature limit at the zero-temperature equilibrium volumes of the structures. The effects of thermal expansion are not reported for simplicity as they are very small, contributing less than $0.01k_{\text{B}}$ to the entropy difference between the DO_{22} and disordered phases at a temperature of 1000 K. The required force constants were fit to *ab initio* calculations of forces in supercells with slightly displaced atoms [32].

The calculations were made computationally feasible by restricting displacements to consist of whole planes of atoms, thereby maintaining as much symmetry as possible. Planar force constants were obtained from the displacements and forces according to the relation

$$-\mathbf{F}^{\alpha}(n) = \sum_{m,\beta} \lambda^{\alpha\beta}(n-m) \mathbf{u}^{\beta}(m) \quad (5)$$

where $\mathbf{F}^{\alpha}(n)$ is the force on atom α in layer n , $\mathbf{u}^{\beta}(m)$ is the displacement of atom β in layer m , and $\lambda^{\alpha\beta}(n-m)$ is the $(n-m)$ th layer planar force constant in the direction normal to the planes. The planar force constants can be related to the more usual force constant matrix between atoms α and β by the formula

$$-\lambda^{\alpha\beta}(n) = \sum_{(\mathbf{R}|\hat{\mathbf{e}} \cdot (\mathbf{R} + \boldsymbol{\tau}_{\alpha\beta}) = d_n)} \mathbf{D}^{\alpha\beta}(\mathbf{R}) \quad (6)$$

where d_n is the distance between the planes being considered, $\hat{\mathbf{e}}$ is the normal vector to the planes, $\boldsymbol{\tau}_{\alpha\beta}$ is the basis vector connecting atoms α and β in a unit cell, and \mathbf{R} is a lattice translation vector. $\mathbf{D}^{\alpha\beta}(\mathbf{R})$ is the usual force constant matrix between atoms α and β , separated by basis vector $\boldsymbol{\tau}_{\alpha\beta}$ and lattice vector \mathbf{R} , which is calculated by second derivatives of the energy with respect to displacements of those atoms. Equation (6) shows that the planar force constants are obtained by collecting the usual force constants for all atoms in the appropriate plane, projecting these force constants along the plane normal, and then summing the resulting terms. By performing calculations along a number of directions and applying symmetry relations it is possible to determine all the desired force constants from equations (5) and (6).

Our *ab initio* calculations were performed within the local density approximation (LDA) using the VASP [33, 34] package, which implements ultra-soft [35] pseudopotentials [36]. To ensure that the errors in the calculated forces did not introduce errors in the vibrational

Table 1. Correlations of the structures used. p_n denotes the n th nearest-neighbour correlation while t_{lmn} denotes a triplet made of overlapping p_l , p_m and p_n pairs.

Structure	p_1	p_2	t_{111}	t_{112}	t_{113}	t_{114}
$L1_2$	0	1	1/2	-1/2	1/2	-1/2
DO_{22}	0	2/3	1/2	-1/6	1/6	1/6
SQS-8	1/4	1/3	-1/4	0	-1/12	-1/6
Random	1/4	1/4	-1/8	-1/8	-1/8	-1/8

entropies that exceed $0.02k_B$, the following parameters were used. The number of k -points in the first Brillouin zone was chosen to be approximately $(14)^3$ divided by the number of atoms in the unit cell. A high energy cutoff of 365 eV was used to accurately determine the equilibrium cell shapes, while a cutoff of 211 eV was sufficient to obtain accurate forces.

Since we were interested in the change in vibrational thermodynamics upon disordering it was necessary to be able to calculate vibrational properties of the disordered phase. The disordered state was modelled by a special quasirandom structure (SQS) [37]. The SQSs are small unit cell structures that are constructed to mimic the short-range correlations of a truly random structure as much as possible. They have been shown to give good estimates of disordered values for a number of electronic [38] and vibrational [26] properties. For this study an eight-atom SQS (SQS-8) is used, which we believe is large enough to accurately represent the vibrational thermodynamics of the disordered lattice, but is small enough to be computationally tractable. A useful way to represent the SQS-8 is in terms of correlations. These are defined as follows. Assign to each lattice site the pseudospin value of -1 or $+1$, depending on whether the site is occupied by a Pd or V, respectively. Any cluster of sites can then be assigned a cluster function, which is simply the product of the pseudo-spin values on all the sites in the cluster. A correlation is a cluster function averaged over all symmetry equivalent clusters in the parent lattice. Structures with similar correlations tend to have atoms in similar environments. The correlations for the SQS-8 used in this work, as well as the $L1_2$, DO_{22} , and a truly random structure, are given in table 1. Note that the correlations for the SQS-8 and random structures are quite similar, showing that the SQS-8 has similar local environments to the disordered phase.

In calculating the force constants some choice must be made about how many to include. Table 2 shows the convergence of the entropy as a function of the number of neighbours included in the force constant matrix. Unfortunately, computational limitations restrict us to including only first-neighbour force constants in the SQS-8 structure. It can be seen that over the first three neighbour shells the total entropy of the $L1_2$ and DO_{22} structures change by about $0.1k_B$, but that the entropy difference between them is converged to within about $0.02k_B$ by the first-neighbour shell. This suggests that the entropy difference between the SQS-8 and DO_{22} structures is probably also well converged after the first-neighbour force constants.

Table 2 shows that the entropy of the disordered phase is $0.07k_B$ below that of DO_{22} . The major sources of error in this result are likely to be the use of the SQS-8 to approximate the disordered phase and the limiting of the force constants to the nearest-neighbour shell. The error due to the SQS-8 can be estimated by considering differences between $L1_2$ and DO_{22} . These two structures have an entropy difference of $0.08k_B$ and correlations that are identical for the first-neighbour shell and fairly close after that. For comparison, the SQS-8 and totally random structures also have identical first-neighbour correlations and farther range correlations that are much more similar than those of $L1_2$ and DO_{22} . It is therefore to be expected that the entropy difference between the SQS-8 and random structure would be significantly less

Table 2. Vibrational entropy in units of k_B as a function of the interaction range included in the spring model. Range is expressed as the number of nearest neighbour shells. Only stretching and bending terms are included for the column labelled 1(sb) (see text).

Structure	1(sb)	1	2	3
$L1_2$	-4.40	-4.39	-4.44	-4.48
DO_{22}	-4.48	-4.47	-4.53	-4.58
SQS-8	-4.53	-4.54		
$L1_2-DO_{22}$	0.08	0.08	0.08	0.10
$SQS-8-DO_{22}$	-0.05	-0.07		

than the $0.08k_B$ entropy difference between $L1_2$ and DO_{22} . Based on the correlations shown in table 1 we estimate the error associated with using the SQS-8 at less than $0.04k_B$. The error due to the use of only nearest-neighbour force constants we believe to be about $0.02k_B$, again based on comparison to the entropy difference between the $L1_2$ and DO_{22} structures. Even if we make a very pessimistic error estimate and base the rate of convergence on the absolute vibrational entropies, rather than their differences, we still get an error less than about $0.1k_B$. Even in the presence of these errors, we can still exclude the possibility that the change in entropy upon disordering is large and positive, which is the most important feature of our calculations.

Indeed, the decrease in vibrational entropy upon disordering is in the opposite direction from what would be expected based on the bond-proportion model discussed above. The reason is that size effects, even in this system with almost no apparent size mismatch, contribute significantly to the vibrational thermodynamics. We argued earlier that a Pd-V bond might behave similarly to a bond between two elements of the middle of the transition metal series, which typically have a larger stiffness. However, elements of the middle of the transition metal series are also characterized by smaller lattice constants. One would then expect Pd-V bonds to be shorter than V-V or Pd-Pd bonds. As we will see, the short Pd-V bond length is indeed at the source of the important relaxations observed in Pd-V. The importance of size effects in this system will be demonstrated by analysing bond strengths and lengths.

Unfortunately, there is no single parameter which represents the strength of the force constants between two atoms, since this is, in general, a nine-element matrix. A great simplification is to represent the force constant matrix in terms of two parameters, a stretching and a bending term. This determination of the stretching and bending terms is done in the following manner. Start by considering a 3×3 force constant matrix between two atoms, represented in cartesian coordinates with one axis along the bond between the atoms. The diagonal terms of the force constant matrix then represent a stretching and two bending terms, which can be reduced to one by requiring the bending terms to be orientation independent. The remaining off-diagonal terms are assumed to be zero.

The ‘reduced’ force constant matrix is thus fully defined by the elements of its diagonal: an element S (stretching), corresponding to the bond direction and two elements B (bending) corresponding to the other two directions. By a simple rotation, the reduced matrix can then be transformed back into the usual cartesian coordinate system. It will no longer be diagonal, but all the elements will still be given by linear functions of S and B . The values of S and B are then determined by fitting (by a least-squares method) the reduced force constant matrices to the forces obtained from *ab initio* calculations, as described at the beginning of section 3.

It is very interesting to note that the entropies calculated with only stretching and bending terms differ by less than $0.01k_B$ from the entropies calculated with the exact nearest-neighbour force constant matrix for all the cases considered (see column 1(sb) in table 2).

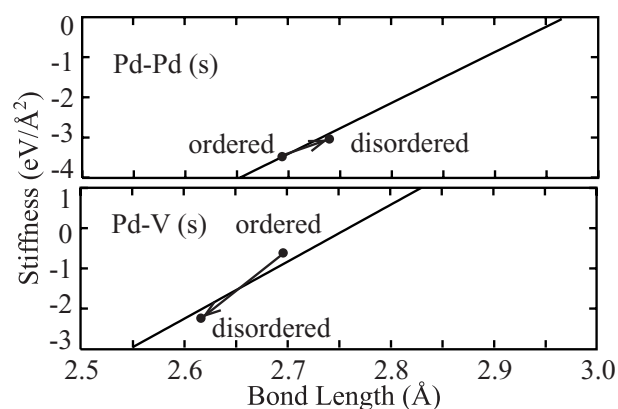


Figure 2. Shift in average stiffness (defined as the spring constant along the stretching direction) and bond length upon disordering. The fitted line of stiffness versus length is shown for reference.

Figure 2 shows the average stiffness of Pd–Pd and Pd–V first-neighbour bonds as a function of their average distance in both the ordered DO_{22} and $L1_2$ structures and the SQS-8. The stiffness here is taken to be the stretching term defined above. No V–V bond results are included as there are very few of those (none in the ordered phases). Figure 2 shows that in disordering there is a significant change in both the Pd–Pd and Pd–V bond lengths. The change in bond lengths occurs because in the ordered phase all the bonds are constrained by symmetry to be the same length, but in the disordered structure the naturally shorter Pd–V bonds can contract and the naturally longer Pd–Pd bonds can expand. As would be expected, when bonds contract (expand) their stiffness increases (decreases). The contraction of the Pd–V bonds is much greater than the expansion of the Pd–Pd bonds and it is this imbalance which leads to an overall stiffening of the disordered phase and the lowering of the entropy with disorder.

The importance of the relaxations can be seen more quantitatively by removing them in an approximate manner. To do this, we use the stretching and bending model discussed above. We take the stretching and bending parameters for each nearest-neighbour bond in the SQS-8 structure and compute an average for each bond type (Pd–Pd, Pd–V and V–V). This averaging is needed because a given type of bond (e.g. Pd–Pd) may have slightly different values of S and B , depending on the bond's local environment. These average Pd–Pd, Pd–V and V–V force constants matrices are an approximation to the ‘true’ force constants we would expect with no symmetry constraints. These force constants are then used to calculate the entropy for both the ordered DO_{22} and SQS-8 structures and the increase in entropy with disordering is found to be $0.26k_B$. This calculation uses a single set of bond length independent force constants for both the ordered and disordered phases and therefore does not include the relaxation differences between the two phases. Without the relaxation effects involved the bond-proportion model applies and the expected entropy increase is seen to occur. Therefore, we conclude that the relaxations are what cause the bond-proportion model to give an incorrect prediction and the vibrational entropy to decrease with disordering.

It can be shown that the stretching and bending force constants are approximately independent of the chemical environment, provided that the proper bond length is used. By this it is meant that a given bond, say Pd–Pd, will have similar values for S and B for a given bond length, whether the Pd–Pd bond is in a $L1_2$, DO_{22} , or SQS structure. This raises the possibility of using the values of S and B determined from simple cases to obtain force constants for a variety of complex chemical environments.

This idea is similar to that explored by Sluiter *et al* [39], where an attempt was made to develop transferable force constants by averaging over configurations. Sluiter *et al* found that the averaged force constants were not able to accurately represent the vibrational free energy of different chemical orderings. They attribute at least part of this problem to violation of invariances that the force constants must satisfy. We believe the approach chosen here may be more accurate than the averaged force constants of Sluiter *et al* for two reasons. Most importantly, the stretching and bending model allows the force constants to depend on bond length, which the work presented in this paper proves to be very important. In addition, by using only the diagonal S and B terms, the force constant matrices automatically satisfy all the invariances associated with crystal symmetry. This should alleviate some of the problems associated with violations of the invariances. Further testing of the stretching and bending model is necessary before its accuracy can be established.

A more detailed discussion of this work on Pd_3V can be found in [25].

4. Embedded-atom method study of Ni_3Al

Ni_3Al is ordered in the $L1_2$ structure essentially up to its melting point at about 1670 K [31], although it is possible to create a metastable disordered phase. There have been a number of experimental [6, 40] and theoretical [19–22, 26] studies of the vibrational thermodynamics of ordered and disordered Ni_3Al . The experiments and calculations have given a range of results for the change in entropy with disordering, probably due to variations in potentials used and differences between the perfect crystals modelled in calculations and those actually obtained in experiment (for further discussion of this, see [12, 22, 41]). In this section we will not focus on the overall change in vibrational thermodynamics between phases, but instead on how the local environment of a given atom affects its vibrational behaviour.

The advantage of a local approach is that it allows one to directly identify how each atom is being influenced by its surroundings. The local vibrational thermodynamics of an atom can be calculated by the following approach. The total density of states, $g(\omega)$, can be written

$$g(\omega) = \sum_{\alpha\kappa} \left[\frac{\Omega}{(2\pi)^3} \right] \sum_j \int d\mathbf{k} |e_\alpha(\kappa; j\mathbf{k})|^2 \delta(\omega - \omega_j(\mathbf{k})) = \sum_{\alpha\kappa} g_{\alpha\kappa}(\omega) \quad (7)$$

where Ω is the volume per atom, α and κ denote a Cartesian direction and atom in the unit cell, and \mathbf{k} and j are the wavevector and branch of each phonon mode. $e_\alpha(\kappa; j\mathbf{k})$ is the value of the eigenvector for mode $j\mathbf{k}$ associate with direction α and atom κ , and $\omega_j(\mathbf{k})$ is the frequency of mode $j\mathbf{k}$. The $g_{\alpha\kappa}(\omega)$ are projected densities of states, and represent how much of the total density of states can be attributed to motion of atom κ in direction α . In this study we will calculate the projected densities of states onto an atom, $g_\kappa(\omega)$, which simply involves summing $g_{\alpha\kappa}(\omega)$ over the possible values of α . Once the projected density of states onto an atom has been calculated the local vibrational thermodynamics can be found in the harmonic approximation by integrating against the appropriate function [42].

All the calculations shown here for Ni_3Al were performed using the embedded-atom method [43–45] with the Foiles and Daw Ni_3Al potential [46]. Calculations are converged to within less than $0.01k_B$ with respect to density of states integration and k -point sampling.

In order to investigate the effects of various local environments the local entropy was calculated for every atom in a randomly decorated 256-atom supercell of Ni_3Al . The entropies were calculated at a temperature of 600 K, which is near the Debye temperature for this material [40]. The local entropies are plotted in figure 3 as a function of the number of Al nearest neighbours for two cases: one where the atoms were forced to remain on their ideal

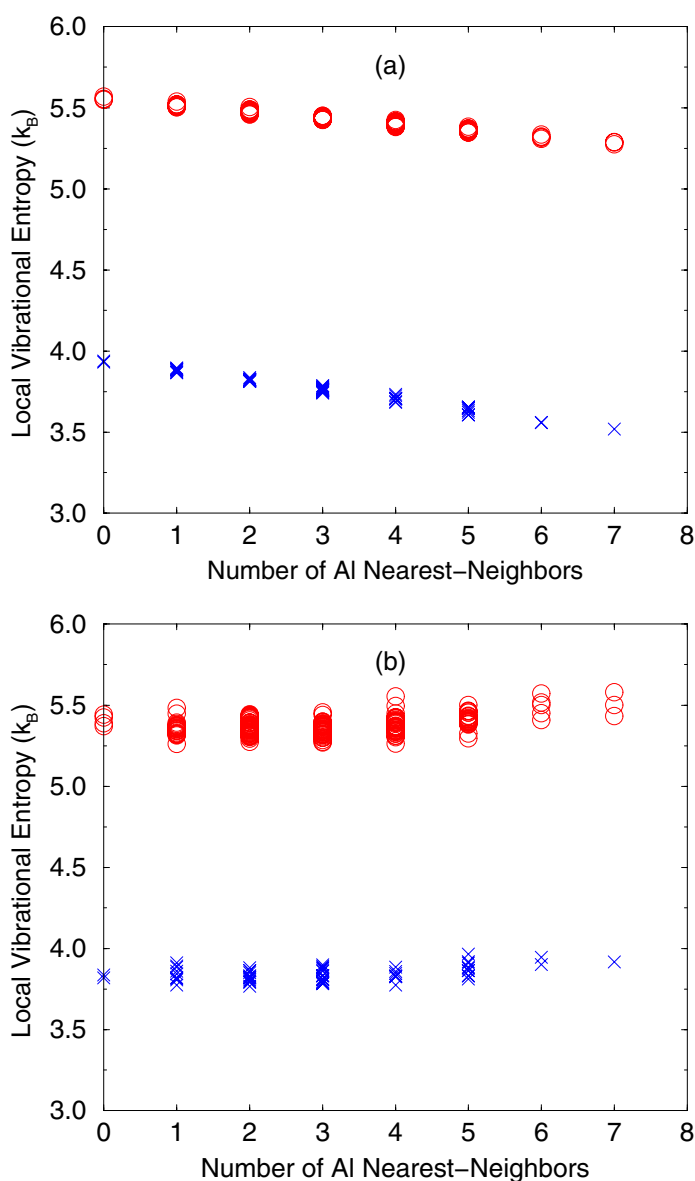


Figure 3. The local entropy for Ni (open circles) and Al (crosses) atoms as a function of the number of Al nearest neighbours, as determined from a disordered configuration. Results are given for the unrelaxed (a) and relaxed (b) structures.

lattice sites and one where the atoms were allowed to relax to their equilibrium positions. All these calculations were done at the equilibrium volume of the unrelaxed disordered phase.

There are two important things to notice about these results. The first is that the Ni atoms have consistently higher local entropies than the Al atoms. There are two contributions to this difference. First, the Al generally have stiffer force constants than the Ni, which tend to decrease the Al entropy relative to the Ni. A somewhat larger effect is that Ni is about 2.2 times as heavy as Al, which again causes it to have a larger vibrational entropy than Al.

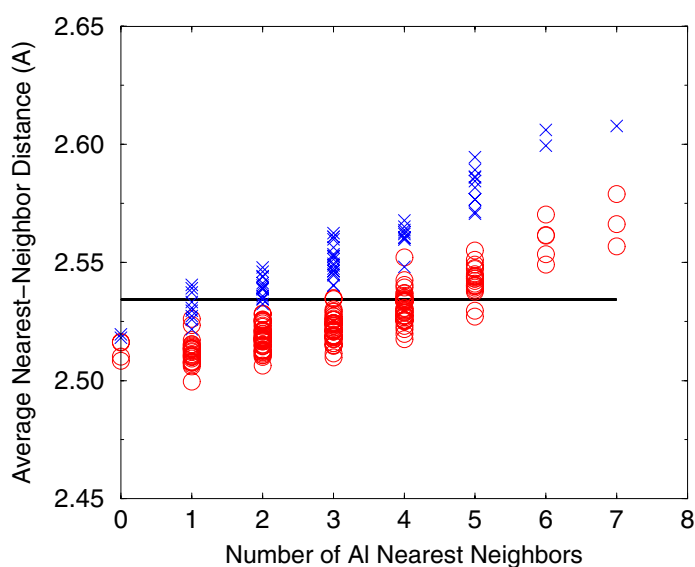


Figure 4. The average nearest-neighbour distance for Ni (open circles) and Al (crosses) atoms as a function of the number of Al nearest neighbours, as determined from a relaxed disordered configuration. The average nearest-neighbour distances for the unrelaxed configuration are given by the solid line.

The other important thing to notice is that the overall behaviour of the entropy as a function of local environment changes dramatically when relaxations are included. When no relaxations are allowed the entropy decreases for both types of atoms as more Al neighbours are included. When relaxations are allowed the entropy becomes much noisier, and seems fairly flat, or even slightly increasing, as a function of the number of Al neighbours. To make sense of these results we need to consider size effects.

The size mismatch between Ni and Al is very large [30]

$$\frac{(V_{\text{Al}} - V_{\text{Ni}})}{(V_{\text{Al}} + V_{\text{Ni}})/2} = 0.41$$

which means that relaxation effects are likely to be very important. Figure 4 shows the average distance to the nearest-neighbour shell for all the atoms as a function of the number of Al nearest-neighbour pairs. For the unrelaxed case the neighbours are always the same distance, but the relaxation allows the neighbours to spread apart more and more as they become predominately made up of large Al atoms. The behaviour of the local entropy can now be understood. When there is no relaxation, replacing Ni neighbours with Al neighbours creates progressively more crowding of the central atom. This leads to compressed bonds, which are stiffer, and the vibrational entropy of the central atom decreases. When relaxation is allowed to take place the large Al atoms can move apart to make more space, the bonds of the central atom are no longer compressed, and the atom's entropy does not decrease with increasing numbers of Al neighbours.

It is interesting to consider the predictions of the bond-proportion model for the local entropy of the unrelaxed case. Ni has a bulk modulus that is more than twice as large as that for Al (the potentials fit the experimental bulk moduli exactly) [46], so based on the pure elements one would expect that the Ni–Ni bonds would be much stiffer than the Al–Al bonds. As more Al atoms are added to the environment of a Ni or an Al one would expect a decrease in the average bond stiffness (because of fewer bonds to Ni) and an increase in vibrational

entropy. These predictions are the opposite of what is seen for the unrelaxed case. The failure of the bond-proportion model is again due to the influence of size effects. Ni_3Al is between pure Ni and pure Al in average lattice parameter, so the Al–Al bonds are compressed and the Ni–Ni bonds are expanded in the unrelaxed lattice. This strain effectively brings the bond stiffness of Al–Al bonds above that of Ni–Ni bonds. If one takes this size induced reversal of bond stiffnesses into account, then the bond-proportion model predicts the correct qualitative behaviour. The change in behaviour that is seen when the system relaxes is due in part to the release of some of the strain in the bonds, making Ni–Ni bonds stiffer and Al–Al bonds less stiff.

Figure 3 shows that the nearest-neighbour environment determines the local entropy quite precisely when there are no relaxations, but relaxations introduce other significant influences on the local thermodynamics. This can be made more quantitative by constructing a local cluster expansion. The cluster expansion formalism [3, 4, 37] is used to represent the dependence of functions of lattice decoration in terms of real-space interactions. In section 3 we defined cluster functions. It can be shown that these form a complete orthonormal basis for functions of lattice decoration. The cluster expansion is just an expansion in the basis of cluster functions. The coefficients for each cluster function are called effective cluster interactions (ECI). Because we are studying local quantities we will make use of a local cluster expansion [26, 41], in which there are somewhat different independent ECI than in the traditional cluster expansion. We make a local cluster expansion by fitting the local entropies for all the 256 atoms in a large disordered cell to ECI for the first eight neighbour shells (there is a point and pair ECI for each shell). The results of this fit, both the ECI and the root-mean-square (RMS) error between the true and fitted entropy values, are shown for both the relaxed and unrelaxed case in figure 5.

The local cluster expansion clearly shows the dramatic influence of relaxations. When no relaxations are present the expansion is dominated by the first-neighbour shell, which can be seen by the large first-neighbour ECI and the very low RMS error obtained with only the first shell. When relaxations are included the ECI become much longer range (the largest ECI is in fact in the fifth-neighbour shell). The introduction of longer-range interactions when relaxations are included has also been found in cluster expansions of the total energy [4, 48–51]. In addition, in the relaxed case the RMS error is almost constant after the fifth-neighbour shell, even though it is about five times as large as the corresponding error in the unrelaxed case. The failure of longer-range pairs to improve the RMS error shows that multisite interactions are contributing to the local entropy in the relaxed case. Furthermore, the ECI go from being primarily negative to primarily positive when the relaxations are included. This is the manifestation in the cluster expansion of the above discussed release of strained bonds with relaxation. Finally, note that the point ECI are generally more important than the pair ECI. Point ECI contribute the same amount to a given atom's local entropy independent of the type of the atom. This means that the vibrations of both Ni and Al are influenced similarly by their environment. This is not consistent with the bond-proportion model where one would expect, for example, a very different influence of an Al neighbour on a Ni than an Al. The dominance of the point ECI is just one more way in which the size effects show their importance.

In this section we have shown that for Ni_3Al the local entropy of an atom is primarily determined by the area in which it is free to move. Without relaxation, large Al neighbours crowd a central atom, inhibiting its vibrations, but when relaxation is allowed the Al spread out and the crowding effect essentially disappears. Without relaxation, the compressed Al–Al and Al–Ni bonds are effectively stiffer than the expanded Ni–Ni bonds, despite the much larger bulk modulus of pure Ni than pure Al. It is clear that the local vibrational thermodynamics of Ni_3Al cannot be understood in terms of a simple bond-proportion model and that the behaviour is dominated by the large size effects.

A more detailed discussion of this work on Ni_3Al can be found in [26].

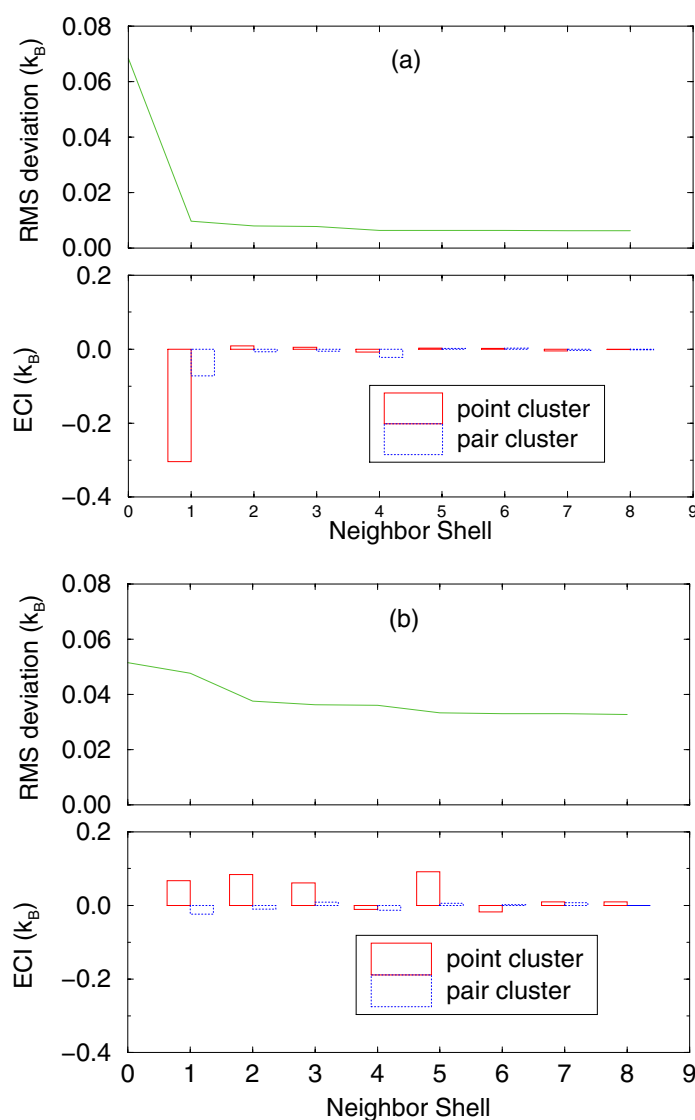


Figure 5. The results of a cluster expansion of the local entropy for an unrelaxed (a) and relaxed (b) disordered configuration. The upper panels show the RMS error in the local entropy values predicted by the ECI compared to the exact calculated values, as a function of the number of neighbour shells in the cluster expansion. The lower panels show the point (full) and pair (broken) ECI for each neighbour shell.

5. Conclusions

This work discusses the importance of size effects in the behaviour of vibrational thermodynamics. We have shown that a simple bond-proportion model, in which each bond type is assumed to have a fixed stiffness, cannot reliably explain the configurational dependence of the vibrational thermodynamics, even for systems with small size mismatch.

First-principles calculations on the Pd_3V system predict that the vibrational entropy decreases by $0.07k_{\text{B}}$ upon disordering the DO_{22} phase. This decrease is explained by the

stiffening of the disordered phase that occurs as the broken symmetry allows the Pd–V bonds to contract.

We have also performed embedded-atom method calculations of the local vibrational entropy for all the individual atoms in a large Ni₃Al supercell. The local entropy, as a function of the number of Al nearest neighbours, decreases when no relaxation is included, but remains fairly flat on average when relaxation is included. This can be explained by the fact that the larger Al atoms crowd a central atom when relaxations are not allowed, but push apart and allow for more vibrations when relaxations are included. A local cluster expansion is performed and shows the increased contributions of long-range and multisite ECI due to the relaxations.

This work highlights the importance of relaxation effects in vibrational studies. Ignoring or treating inaccurately the relaxation effects can lead to errors of a qualitative nature, even for systems with very small size mismatch. This problem is particularly challenging for those involved in first-principles research, where accounting for the dependence of the force constants on the magnitude of the local relaxations can come at a high computational cost. This work does suggest some methods by which relaxation effects can be included in a computationally tractable manner. The use of the stretching and bending model, with the force constants parametrized as a function of bond length, seems to give very accurate results and could effectively provide transferable force constants to allow calculations for very complex unit cells. This approach is presently under further development.

Acknowledgments

This work was supported by the Department of Energy, Office of Basic Energy Sciences under Contract Nos DE-FG02-96ER45571, DE-AC03-76SF00098 and DE-AC04-94AL85000. This work was also supported by NSF cooperative agreement ACI-9619020 through computing resources provided by the National Partnership for Advanced Computational Infrastructure (NPACI) at the San Diego Supercomputing Centre. Axel van de Walle acknowledges support from a '1967' scholarship from the Natural Sciences and Engineering Research Council of Canada. The authors wish to thank G Garbulsky and S M Foiles for providing computer programs which made this work possible. The authors would also like to thank M D Asta for stimulating discussions.

References

- [1] de Fontaine D 1979 *Solid State Phys.* **34** 73
- [2] Ducastelle F 1991 Order and phase stability in alloys *Cohesion and Structure* vol 3 (The Netherlands: North-Holland)
- [3] de Fontaine D 1994 *Solid State Phys.* **47** 33
- [4] Zunger A 1994 Statics and dynamics of alloy phase transformations *NATO ASI Series. Series B, Physics* vol 319, ed P E A Turchi and A Gonis (New York: Plenum) p 361
- [5] Nagel L J 1996 *PhD Thesis* California Institute of Technology
- [6] Fultz B et al 1995 *Phys. Rev. B* **52** 3315
- [7] Anthony L, Nagel L J, Okamoto J K and Fultz B 1994 *Phys. Rev. Lett.* **73** 3034
- [8] Nagel L J, Anthony L and Fultz B 1995 *Phil. Mag. Lett.* **72** 421
- [9] Nagel L J, Fultz B, Robertson L J and Spooner S 1997 *Phys. Rev. B* **55** 2903
- [10] Fultz B et al 1995 *Phys. Rev. B* **52** 3280
- [11] Nagel L J, Fultz B and Robertson J L 1997 *Phil. Mag.* **75** 681
- [12] Bogdanoff P D and Fultz B 1999 *Phil. Mag.* **79** 753
- [13] Garbulsky G D 1996 *PhD Thesis* Massachusetts Institute of Technology
- [14] Garbulsky G D and Ceder G 1994 *Phys. Rev. B* **49** 6327
- [15] Garbulsky G D and Ceder G 1994 *Phys. Rev. B* **53** 8993

- [16] Tepesch P D *et al* 1996 *J. Am. Ceram. Soc.* **49** 2033
- [17] Tseng W T and Stark J P 1994 *Phil. Mag.* B **70** 919
- [18] Cleri F and Rosato V 1993 *Phil. Mag. Lett.* **67** 369
- [19] Ackland G J 1994 *Alloy Modelling and Design* ed G Stocks and P Turchi (Pittsburgh, PA: Minerals, Metals and Materials Society) pp 149–53
- [20] Althoff J D *et al* 1997 *Phys. Rev. B* **56** R5705
- [21] Ravelo R *et al* 1998 *Phys. Rev. B* **57** 862
- [22] van de Walle A, Ceder G and Waghmare U V 1998 *Phys. Rev. Lett.* **80** 4911
- [23] Ozoliņš V, Wolverton C and Zunger A 1998 *Phys. Rev. B* **58** R5897
- [24] Shaojun L, Suqing D and Benkun M 1998 *Phys. Rev. B* **58** 9705
- [25] van de Walle A and Ceder G 2000 First-principles computation of the vibrational entropy of ordered and disordered Pd₃V *Phys. Rev. B* **61**
- [26] Morgan D, Althoff J D and de Fontaine D 1998 *J. Phase Equilibria* **19** 559
- [27] Maradudin A A, Montroll E W and Weiss G H 1971 *Theory of Lattice Dynamics in the Harmonic Approximation* 2nd edn (New York: Academic)
- [28] Wojtowicz P J and Kirkwood J G 1960 *J. Chem. Phys.* **33** 1299
- [29] Gale J D 1991–8 *GULP (General Utility Lattice Program)* version 1.2 (London: Royal Institution of Great Britain and Imperial College)
- [30] Pearson W B, Villars P and Calvert L 1985 *Pearson's Handbook of Crystallographic Data for Intermetallic Phases* (Metals Park, OH: Americal Society for Metals)
- [31] 1990 *Binary Alloy Phase Diagrams* ed B Massalski *et al* (New York: ASM International) 2nd edn
- [32] Wei S and Chou M Y 1992 *Phys. Rev. Lett.* **69** 2799
- [33] Kresse G and Furthmüller J 1996 *Phys. Rev. B* **54** 11 169
- [34] Kresse G and Furthmüller J 1996 *Comp. Mat. Sci.* **6** 15
- [35] Vanderbilt D 1990 *Phys. Rev. B* **41** 7892
- [36] Phillips J C and Kleinman L 1959 *Phys. Rev.* **116** 287
- [37] Zunger A, Wei S-H, Ferreira L and Bernard J E 1990 *Phys. Rev. Lett.* **65** 353
- [38] Hass K C, Davis L C and Zunger A 1990 *Phys. Rev. B* **42** 375
- [39] Sluiter M H, Weinert M and Kawazoe Y 1999 *Phys. Rev. B* **59** 4100
- [40] Anthony L, Okamoto J K and Fultz B 1993 *Phys. Rev. Lett.* **70** 1128
- [41] Morgan D 1998 *PhD Thesis* University of California Berkeley
- [42] Callaway J 1974 *Quantum Theory of the Solid State* student edn (San Diego, CA: Academic)
- [43] Daw M S and Baskes M I 1984 *Phys. Rev. B* **29** 6443
- [44] Foiles S M, Baskes M I and Daw M S 1986 *Phys. Rev. B* **33** 7983
- [45] Daw M S, Foiles S M and Baskes M I 1993 *Mater. Sci. Rep.* **9** 251
- [46] Foiles S M and Daw M S 1987 *J. Mater. Res.* **2** 5
- [47] Sanchez J M, Ducastelle F and Gratias D 1984 *Physica A* **128** 334
- [48] Laks D B, Ferreira L G, Froyen S and Zunger A 1992 *Phys. Rev. B* **46** 12 587
- [49] Wolverton C and Zunger A 1997 *Comp. Math. Sci.* **8** 107
- [50] Wolverton C, Ozolins V and Zunger A 1998 *Phys. Rev. B* **57** 4332
- [51] Ozolins V, Wolverton C and Zunger A 1998 *Phys. Rev. B* **57** 6427